Supporting Information

Organic-Site-Dominated Cooperative Catalysis in Defect-Tolerant 2D Lanthanide MOFs for Direct CO_2 Valorization and DFT Calculations

Yang Fei,[a] Qingjuan Lei,[a] Liming Fan,[a] Tuoping Hu,[a] Qi-Pin Qin,[b] and Xiutang Zhang[a,*]

[a]*School of Chemistry and Chemical Engineering, North University of China, Taiyuan 030051, P. R. China.* [b]*Guangxi Key Lab of Agricultural Resources Chemistry and Biotechnology, College of Chemistry and Food Science, Yulin Normal University, Yulin, 537000, PR China. Contact Email: xiutangzhang@163.com*

Contents

Experimental section

Materials and General Methods. All chemical reagents were commercially obtained from Jinan Henghua Sci. & Tec. Co. Ltd. without any further purification. The infrared spectrum (IR) in the range of 500-4000 cm^{-1} was measured on TENSOR27 spectrometer. XPS spectra were collected on a Thermo Scientific Escalab 250Xi spectrometer. Thermogravimetric analyses (TGA) were performed under nitrogen condition from room temperature to 800 °C on a thermogravimetric analyzer (model NETZSCH STA 209 F3). Powder X-ray diffraction (PXRD) was collected for 2θ values on Rigaku Smartlab (9 KW) diffractometer with Cu K_α radiation. Single-component gas sorption measurements were carried out by an ASAP 2020 Plus instrument. Fluorescence spectra is operated using a Hitachi F-4600 fluorescence spectrophotometer at room temperature. The cryogenic N_2 and CO_2 adsorption and adsorption-desorption isotherms are measured on an ASAP 2020 Plus instrument. The catalytic yield was monitored and analyzed on a Thermo Fisher Trace ISQ GC/MS instrument. ^{1}H NMR spectra were collected on a BRUKER-ASCEnd^{TM} 400 instrument in DMSO-d_6 with *n*-dodecane as the internal standard. Inductively coupled plasma (ICP) measurements were measured on an IRIS Advantage spectrometer.

X-ray crystallography. The diffraction intensity data for **NUC-151** was obtained at 296(2) K using a Bruker Smart-APEX II CCD area detector (Mo-K_α radiation, λ = 0.071073 nm) with graphite-monochromated radiation. The reflection data was consequently corrected for empirical absorption corrections and Lorentz and polarization effects. The structure was solved by direct methods and refined by full-matrix least-squares using the SHELXL package. All non-hydrogen atoms were refined anisotropically. Hydrogen atoms except those on water molecules were generated geometrically with fixed isotropic thermal parameters, and included in the structure factor calculations. The block of SQUEEZE in PLATON was employed to eliminate the highly disordered solvent molecular. The solvent content of **NUC-151** was determined by the thermogravimetric analysis and elemental analysis. Crystallographic data and refinement parameters for **NUC-151** were given in Table S1. Selected bond lengths and angles for **NUC-151** were listed in Table S2. Further details on the crystal structure investigations could be obtained from the Cambridge Crystallographic Data Centre with the depository number CCDC-2492511.

DFT calculation. In this work, we employed a cluster model extracted from the periodic structure and saturated with protons to represent the catalytic active site. All computational tasks—including transition state (TS) searches, geometry optimizations, and vibration frequency analyses—were performed using the DMol3 module within the Materials Studio software package. The electronic structure calculations utilized the Becke, Three-parameter, Lee-Yang-Parr (BLYP) generalized gradient approximation (GGA) functional combined with a double numerical plus polarization (DNP) and DFT Semi-core Pseudopots (DSPP) basis set. To ensure numerical accuracy, energy convergence thresholds for the self-consistent field (SCF) iterations were set to 1.0×10^{-5} Hartree (Ha), while geometric convergence criteria were tightened to 2×10^{-5} Ha, 4×10^{-3} Ha and 5×10^{-3} Å for energy, force and displacement, respectively. Transition states were identified by verifying the presence of a single imaginary frequency in vibration mode analyses, confirming their correspondence to the reaction coordinate.

Table S1. Crystallographic data and refinement parameters of **NUC-151.**

Complex	**NUC-151**
Formula	$C_{33}H_{28}N_4O_{11}Tm$
Mr	825.52
Crystal system	monoclinic
Space group	$P2_1/c$
a (Å)	15.9540(5)
b (Å)	13.8266(3)
c (Å)	17.3140(3)
α (°)	90
β (°)	101.157(2)
γ (°)	90
V(Å^3)	3981.97(16)
Z	4
Dcalcd(g·cm^{-3})	1.377
μ(mm^{-1})	2.284
GOF	1.022
R_1 [I＞2σ(I)][a]	0.0501
wR_2 [I＞2σ(I)][b]	0.1375
R_1[a] (all data)	0.0638
wR_2[b] (all data)	0.1535
R_{int}	0.0363
[a] $R_1 = \sum \| \|F_o\| - \|F_c\| \| / \sum \|F_o\|$. [b] $wR_2 = \| \sum w(\|F_o\|^2 - \|F_c\|^2) \| / \sum \| w(F_o^2)^2 \|^{1/2}$	

Table S2. Selected bond lengths and angles of **NUC-151.**

Tm1-O1	2.432(4)	Tm1#1-O2	2.380(4)	Tm1-O2	2.747(4)
Tm1-O5	2.356(4)	Tm#2-O6	2.355(4)	Tm1#1-O7	2.456(4)
Tm1-O8	2.509(4)	Tm1-O9	2.423(4)		
O1-Tm1-O2	49.79(13)	O1-Tm1-O7#3	141.08(15)	O1-Tm1-O8#3	150.91(14)
O1-Tm1-O10	72.93(16)	O2#2-Tm1-O1	124.32(13)	O2#2-Tm1-O2	75.00(13)
O2#2-Tm1-O7#3	80.08(14)	O2#2-Tm1-O8#3	78.06(14)	O2#2-Tm1-O9	141.82(15)
O2#2-Tm1-O10	141.53(14)	O5-Tm1-O1	78.98(14)	O5-Tm1-O2#2	75.05(13)
O5-Tm1-O2	69.43(12)	O5-Tm1-O7#3	79.60(13)	O5-Tm1-O8#3	128.29(12)
O5-Tm1-O9	143.07(16)	O5-Tm1-O10	75.70(15)	O6#2-Tm1-O1	90.27(14)
O6#2-Tm1-O2	69.50(12)	O6#2-Tm1-O2#2	74.71(13)	O6#2-Tm1-O5	133.78(12)
O6#2-Tm1-O7#3	127.57(14)	O6#2-Tm1-O8#3	77.36(13)	O6#2-Tm1-O9	74.78(15)
O6#2-Tm1-O10	143.41(14)	O7#3-Tm1-O2	144.17(12)	O7#3-Tm1-O8#3	52.60(13)
O8#3-Tm1-O2	141.59(13)	O9-Tm1-O1	78.07(16)	O9-Tm1-O2	114.30(15)
O9-Tm1-O7#3	101.23(16)	O9-Tm1-O8#3	73.32(16)	O9-Tm1-O10	70.11(17)
O10-Tm1-O2	116.51(16)	O10-Tm1-O7#3	70.49(16)	O10-Tm1-O8#3	101.62(17)
Symmetry transformations used to generate equivalent atoms: #1: 1 – X, –1/2 + Y, –1/2 – Z; #2: 1 – X,2 – Y, –Z; #3: +X,3/2 – Y,1/2 + Z.					

Table S3. Cycloaddition reaction of CO_2 with styrene oxide under various conditions.[a]

Entry	NUC-151a (mol %)	*n*-Bu_4NBr (mol %)	Press. (MPa)	Temp. (°C)	Time (h)	Yield (%)[b]
1	−	1.0	1.0	85	4	32
2	−	2.5	1.0	85	4	39
3	−	3.5	1.0	85	4	43
4	−	4.5	1.0	85	4	46
5	0.10	−	1.0	85	4	28
6	0.10[c]	1.0	1.0	85	4	78

[a] Reaction conditions: solvent-free, 20 mmol CE.

[b] The product yield was checked by GC−MS spectrometer with *n*-dodecane as internal standard.

[c] 0.10 mol % **NUC-151**.

Table S4. Cycloaddition reaction of CO_2 with styrene oxide under other cocatalysts.[a]

Entry	NUC-151a (mol %)	cocatalyst	Press. (MPa)	Temp. (°C)	Time (h)	Yield (%)[b]
1	0.10	*n*-Bu_4NBr	1.0	85	4	99
2	0.10	*n*-Bu_4NCl	1.0	85	4	89
3	0.10	*n*-Bu_4NI	1.0	85	4	99
4	0.10	PPNCl	1.0	85	4	92

[a] Reaction conditions: solvent-free, 20 mmol CE, cocatalyst (1.0 mol %).

[b] The product yield was checked by GC−MS spectrometer with *n*-dodecane as internal standard.

Table S5. Comparison of the catalytic activity of various MOFs for the cycloaddition of CO_2 with epoxides.

Series No.	Catalyst	Epoxide[a]	Catalyst (mol%)	Time (h)	Pressure (MPa)	Temp. (℃)	Yield (%)	TON[b]	TOF[c]	Ref.
1	LCU-606	SO	0.6	10	0.1	60	99	165	16.5	S1
2	PY-FO-Br	SO	0.05	20	1	100	78	1560	78	S2
3	JLU-Liu21	SO	0.25	48	0.1	80	92	368	7.7	S3
4	TYUT-13a	SO	0.3	4	0.1	65	87	290	72.5	S4
5	MIL-101-N($Bnme_2$)Br	SO	0.93	5	1.4	100	76	81.5	16.3	S5
6	$\{[Cu_2(L^{4-})(H_2O)_2]\cdot 4DMA\cdot 2H_2O\}_n$	SO	0.4	12	0.1	60	99	248	20	S6
7	CSMCRI-25	SO	0.2	4	0.4	45	>99	645	161	S7
8	Cu-URJC-8	SO	1	24	1.2	25	47	47	1.9	S8
9	Cd-MOF	SO	0.25	4	0.5	50	99.9	399.6	99.9	S9
10	**NUC-151a**	**SO**	**0.1**	**4**	**1**	**85**	**97**	**970**	**242**	**this work**

[a]styrene oxide (SO)

[b]TON (turnover number) = mole of product/mole of catalyst.

[c]TOF (turnover frequency) = TON/time

Table S6. The reaction energy for PO and CO_2 to PC over **NUC-151a** catalysts.

	Total Energy (Ha)	**Energy (Ha)**	**Energy (Kcal/mol)**
Br^-	–344.032131		
CO_2	–188.6715115		
PO	–193.14088		
TmO_6 units	–2465.522628		
Int0	–3002.695639		
Int1	–3002.73218	–0.0365412	–22.92996841
TS1	–3002.721358	–0.0257184	–16.13855318
Int2	–3002.767802	–0.0721625	–45.28269038
TS2	⁻3191.417614	⁻0.050463	⁻31.66603713
Int3	⁻3191.436062	⁻0.0689114	⁻43.24259261
TS3	⁻3191.428491	⁻0.0613401	⁻38.49152615
Int4	⁻3191.456493	–0.0893422	–56.06312392
COOH units	–2466.113134		
Int0	⁻3003.286145		
Int1	⁻3003.353763	⁻0.0676175	⁻42.43065743
TS1	⁻3003.346256	⁻0.0601107	⁻37.72006536
Int2	⁻3003.361848	⁻0.0757023	⁻47.50395027
TS2	⁻3192.001693	⁻0.0440359	⁻27.63296761
Int3	⁻3192.026582	⁻0.0689254	⁻43.25137775
TS3	⁻3192.009464	⁻0.0518072	⁻32.50953607
Int4	⁻3192.061053	⁻0.1033964	⁻64.88227496
NH_2 units	–2465.522628		
Int0	–3002.695639		
Int1	⁻3002.761826	⁻0.0661878	⁻41.53350638
TS1	⁻3002.753108	⁻0.0574691	⁻36.06243494
Int2	⁻3002.763541	⁻0.067902	⁻42.60918402
TS2	⁻3191.415402	⁻0.0482516	⁻30.27836152
Int3	⁻3191.436385	⁻0.0692347	⁻43.4454666
TS3	⁻3191.427868	⁻0.0607179	⁻38.10108943
Int4	⁻3191.472941	⁻0.105791	⁻66.38491041

Total energy of Int0 = Br^- + PO + MOF. Calculation of energy: Int1 = Int1 – Int0; TS1 = TS1 – Int0; Int2 = Int2 – Int0; TS2 = TS2 – CO_2 – Int0; Int3 = Int3 – CO_2 – Int0; TS3 = TS3 – CO_2 – Int0; Int4 = Int4 – CO_2 – Int0.

Table S7. Molecular sizes of epoxides with different substituted groups.

Entry	Epoxides	Molecular Size (Å^3)
1	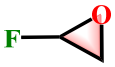	5.81 × 4.85 × 4.46
2	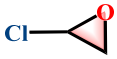	6.37 × 4.87 × 4.57
3		6.26 × 4.85 × 4.54
4	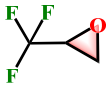	6.70 × 5.34 × 5.40
5	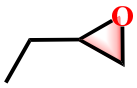	7.24 × 5.70 × 4.97
6	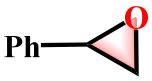	9.20 × 6.98 × 4.80
7	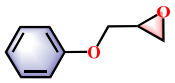	11.29 × 7.13 × 4.80
8	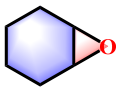	6.70 × 6.95 × 5.10
9	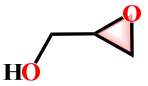	6.89 × 5.37 × 4.96

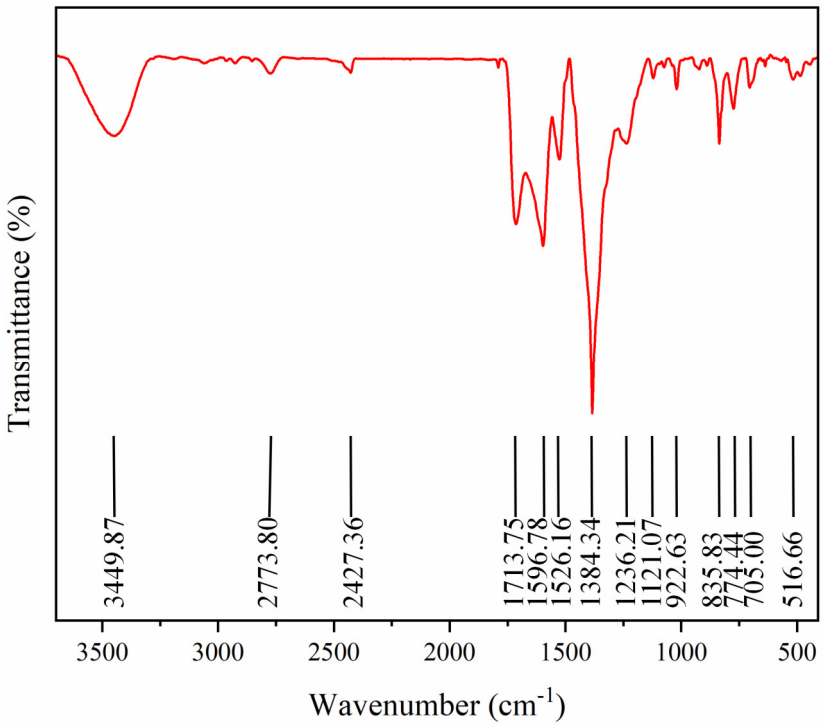

Figure S1. IR spectrum of as-synthesized **NUC-151.**

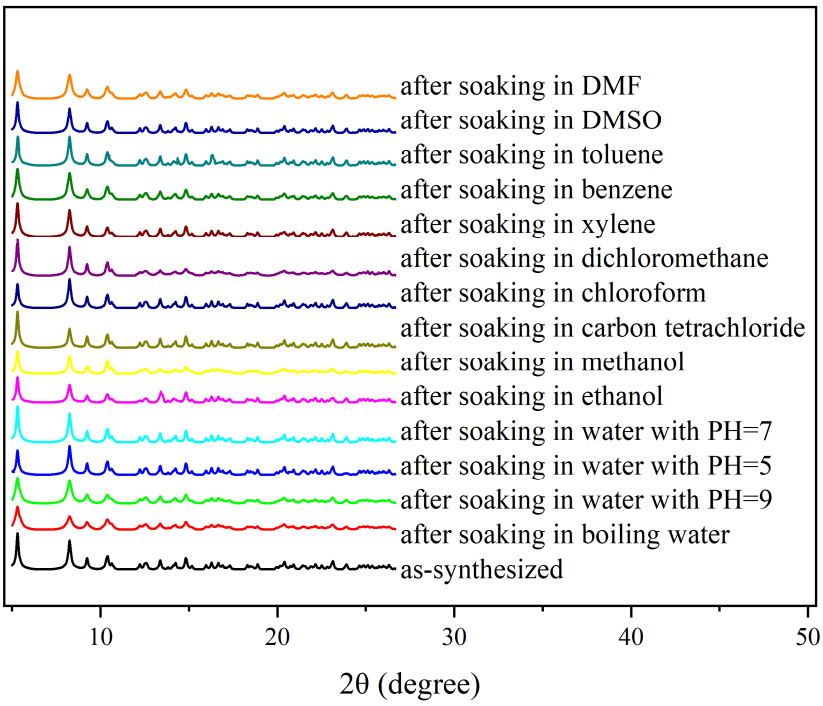

Figure S2. PXRD patterns of all recovered **NUC-151** samples.

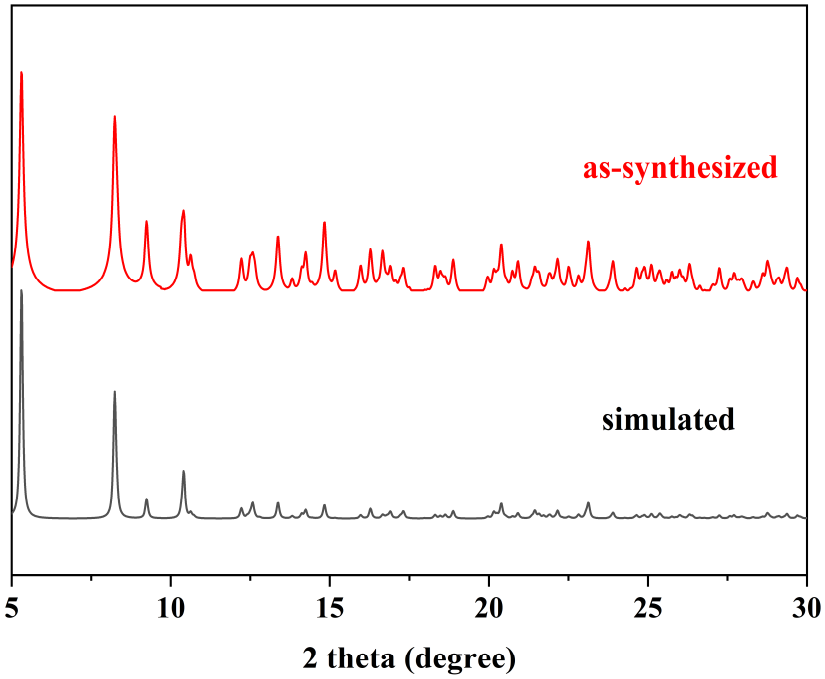

Figure S3. PXRD patterns of as-synthesized **NUC-151** sample.

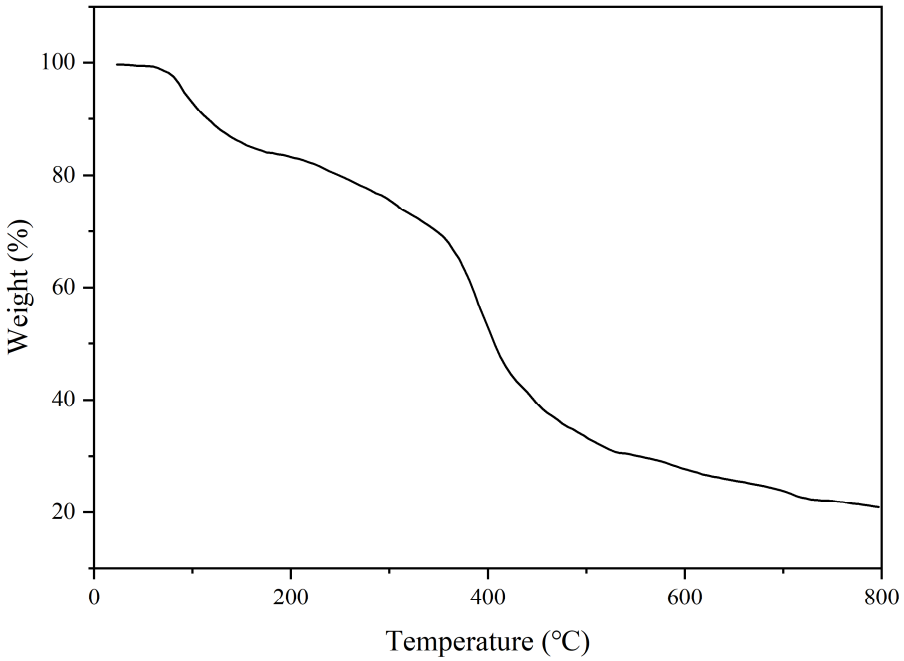

Figure S4. TGA curve of **NUC-151**.

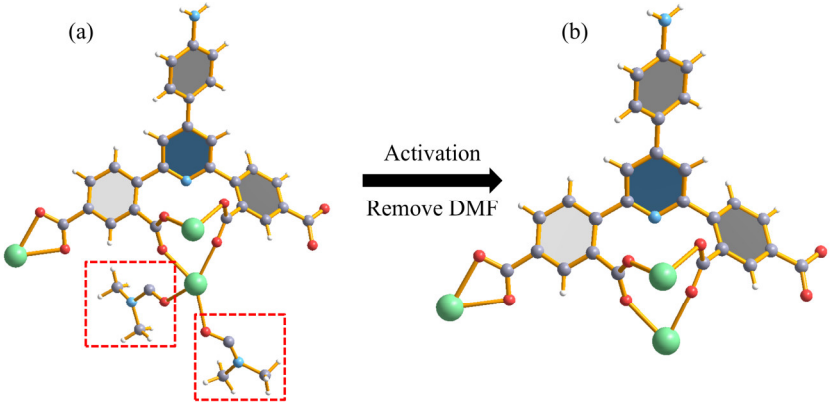

Figure S5. The activation result of **NUC-151a**.

.

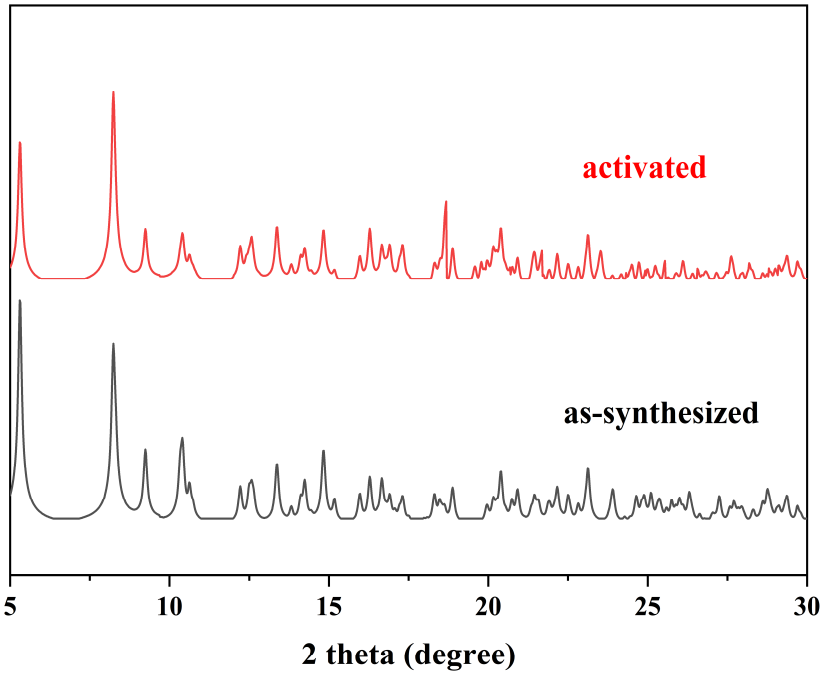

Figure S6. The PXRD patterns of as-synthesized and activated **NUC-151** catalyst.

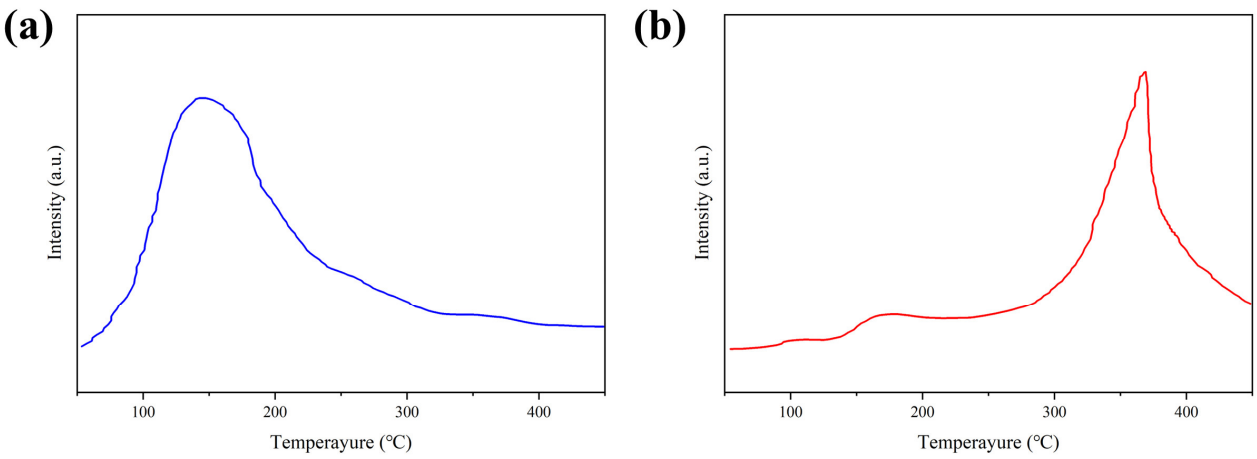

Figure S7. NH_3-TPD (a) and CO_2-TPD (b) profiles of **NUC-151a**.

Isosteric Heat Calculation.

The Q_{st} value is a parameter that describes the average enthalpy of adsorption for an adsorbing gas molecule at a specific surface coverage and is usually evaluated using two or more adsorption isotherms collected at similar temperatures. The zero-coverage isosteric heat of adsorption is evaluated by first fitting the temperature-dependent isotherm data to a virial-type expression, which can be written as:

$$lnP = lnN + \frac{1}{T}\sum_{i=0}^{m} a_i N^i + \sum_{i=0}^{n} b_i N^i$$

$$Q_{st} = -R\sum_{i=0}^{m} a_i N^i$$

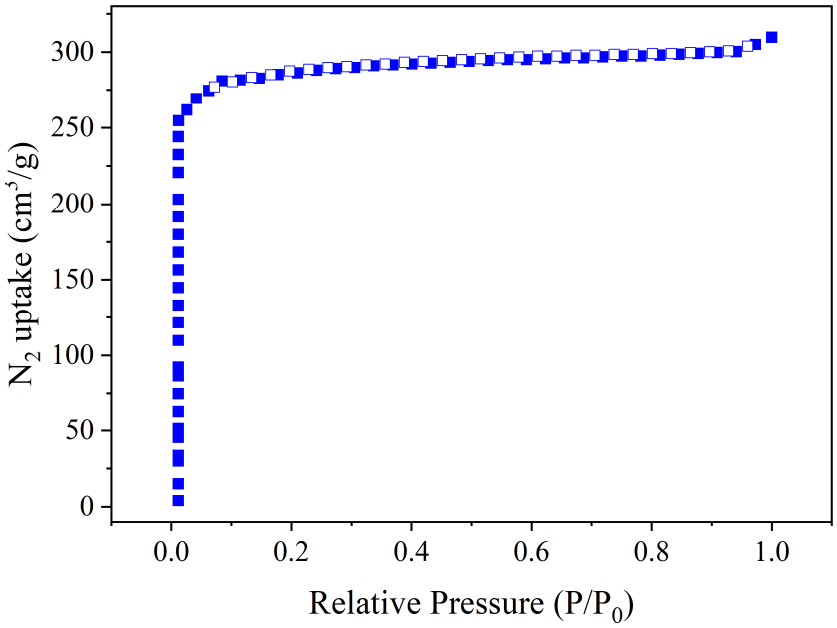

Figure S8. N_2 absorption and desorption isotherms of **NUC-151a** at 77 K.

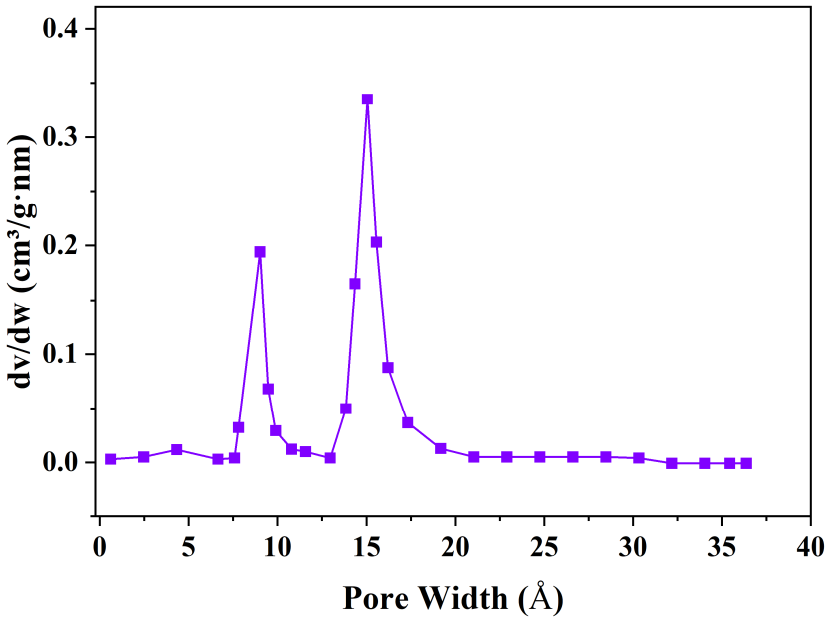

Figure S9. The pore size distribution of **NUC-151a.**

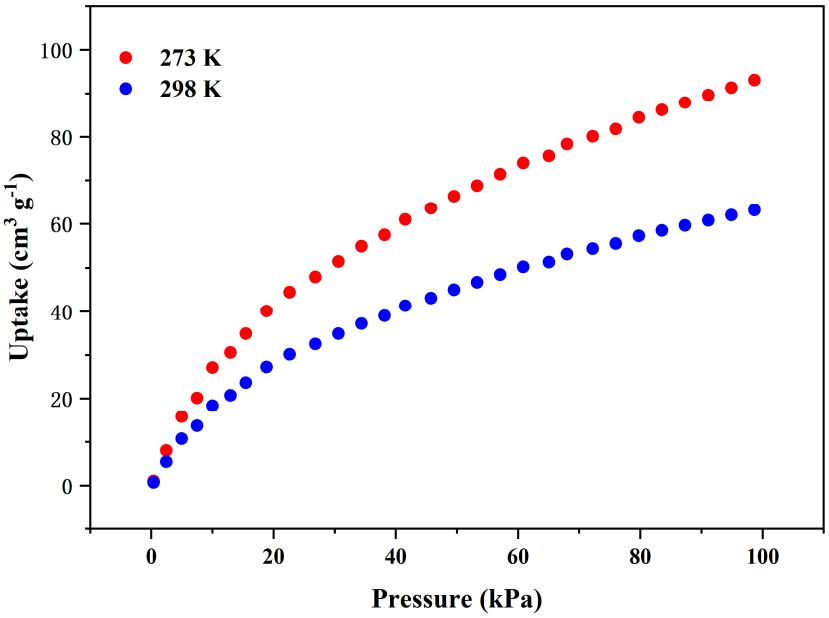

Figure S10. CO_2 adsorption curves of **NUC-151a** at 273 K and 298 K.

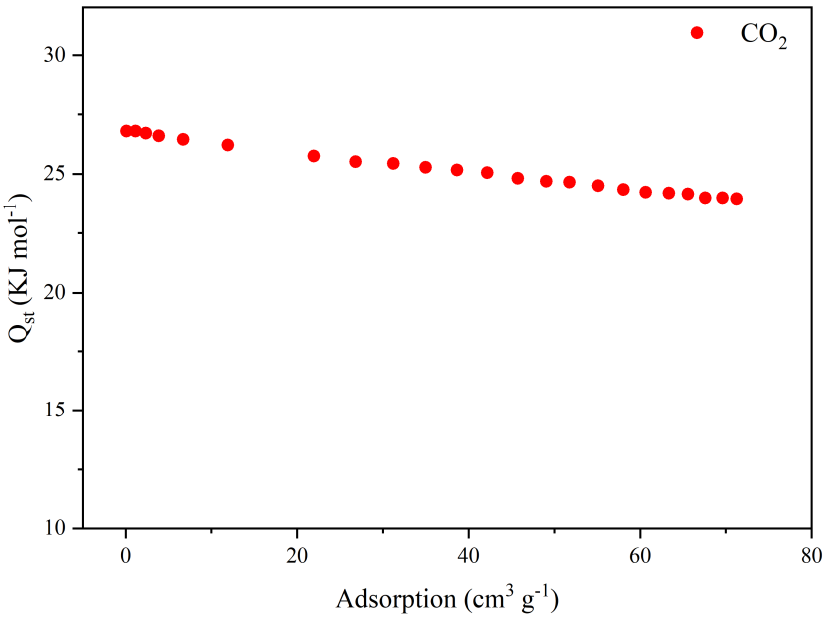

Figure S11. The CO_2 adsorption heat of **NUC-151a.**

Yield Calculation Based on the GC-MS Analysis.

Gas chromatography mass spectrometry (GC-MS) analyses were performed on a time-of-flight Thermo Fisher Trace ISQ GC/MS instrument, the yield (%) was calculated based on the consumption of starting material using the equation:

$$Yield\ (\%) = \left(\frac{\frac{area\ of\ reactant\ at\ 0\ hour}{area\ of\ interal\ standard\ at\ 0\ hour} - \frac{area\ of\ reactant\ at\ any\ time}{area\ of\ interal\ standard\ at\ any\ time}}{\frac{area\ of\ reactant\ at\ 0\ hour}{area\ of\ interal\ standard\ at\ 0\ hour}} \right) \times 100\%$$

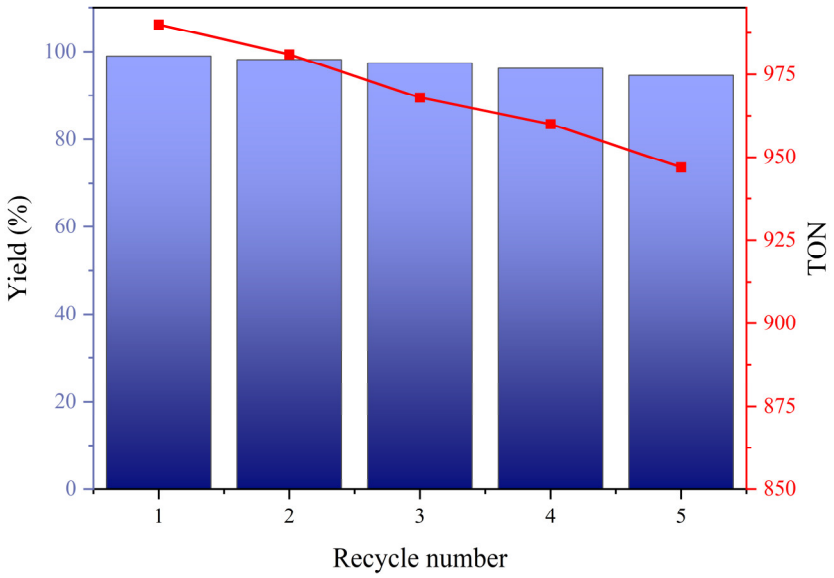

Figure S12. Recyclability study and TON of **NUC-151a** in cycloaddition reaction.

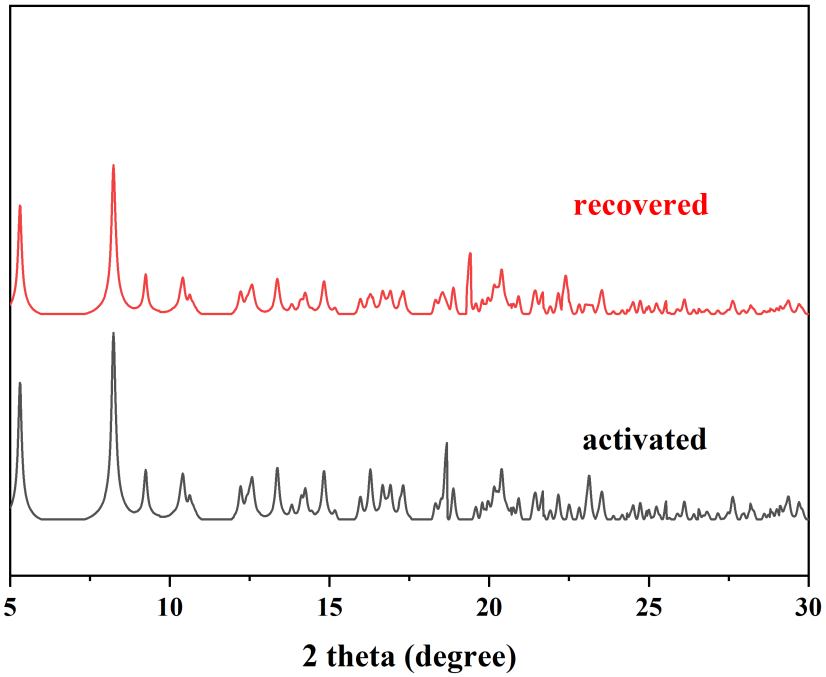

Figure S13. The PXRD patterns of **NUC-151a** before and after catalytic reactions.

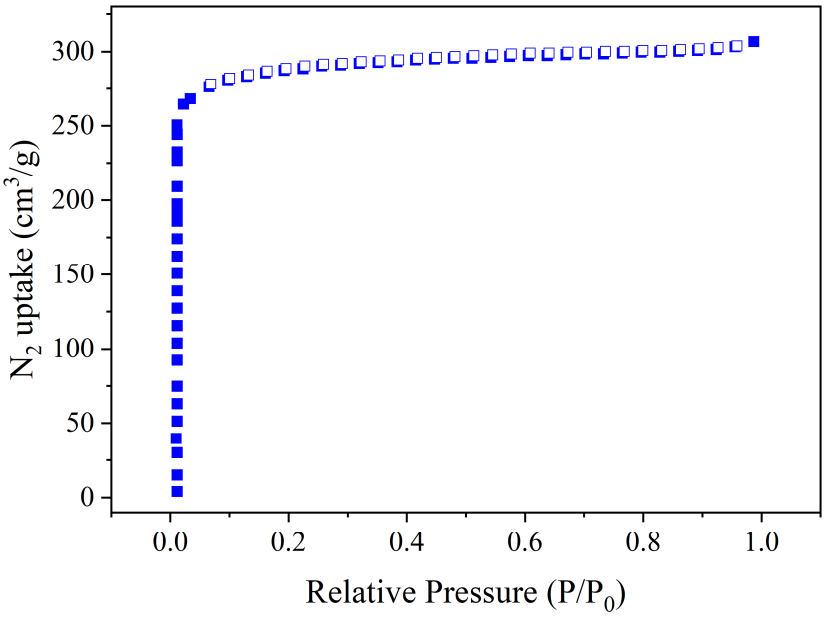

Figure S14. N_2 absorption and desorption isotherms of **NUC-151a** at 77 K after catalytic reactions.

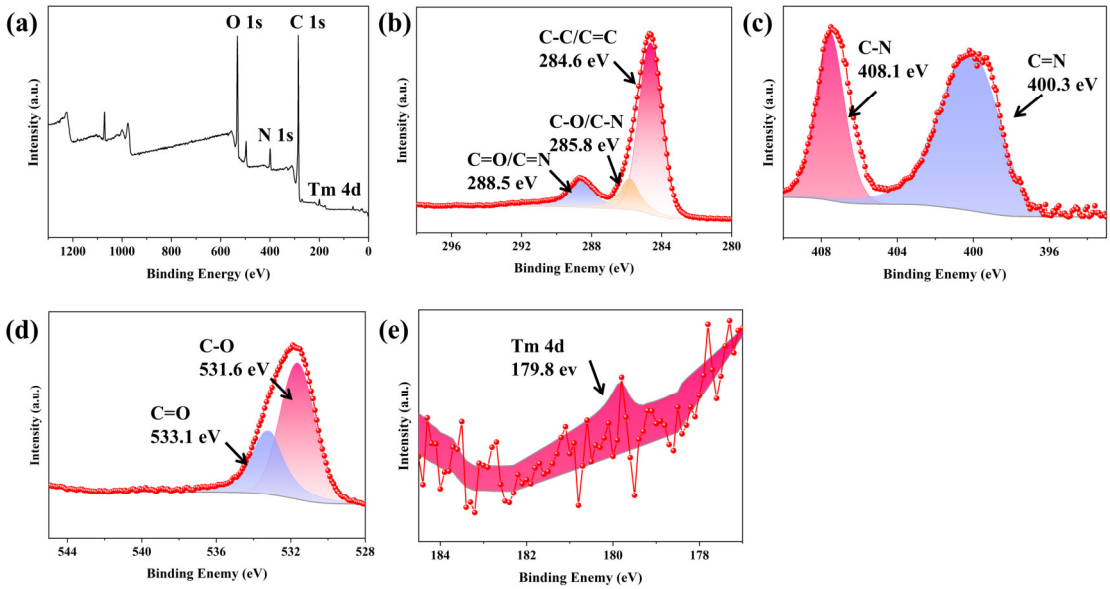

Figure S15. XPS survey spectra of **NUC-151a** after catalytic reactions(d), XPS spectra of C, N, O, Tm, respectively (e–h), in **NUC-151a**.

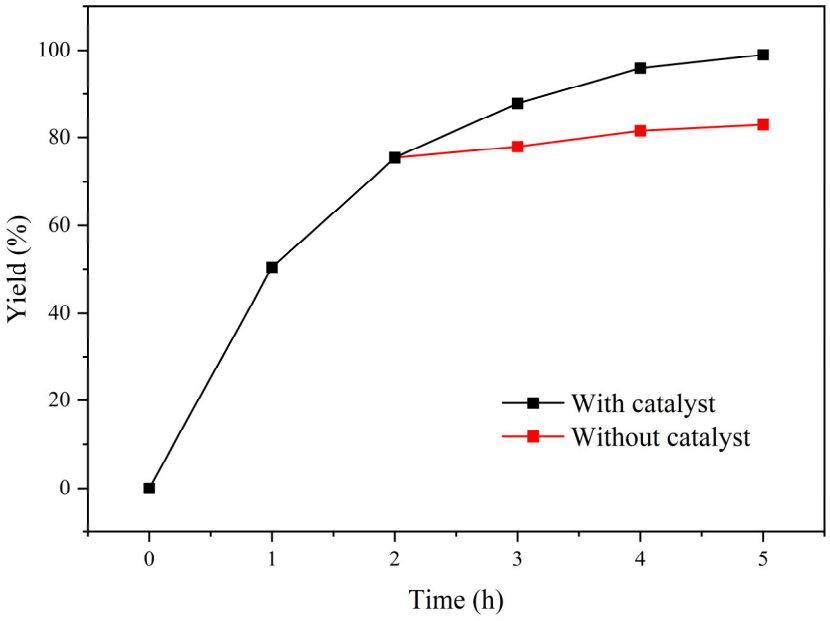

Figure S16. Hot filtrate experiments of the cycloaddition catalyzed by **NUC-151a**.

Reference

[S1] A. Xu, Z. Chen, L. Jin, B. Chu, J. Lu, X. He, Y. Yao, B. Li, L. Dong, M. Fan, *Appl. Catal. A* **2021**, *624*, 118307.

[S2] X. Wang, B. Fan, J. Chen, J. Du, D. Pan, *RSC Adv.* **2025**, *15*, 21914–21921.

[S3] J. Tapiador, P. Leo, F. Gándara, G. Calleja, G. Orcajo, *J. CO_2 Util.* **2022**, *64*, 102166.

[S4] M. Singh, P. P. Mondal, S. Rajput, S. Neogi, *Inorg. Chem. Front.* **2023**, *10*, 3605–3620.

[S5] X. Si, Q. Yao, X. Pan, X. Zhang, C. Zhang, Z. Li, W. Duan, J. Hou, X. Huang, *Inorg. Chem.* **2023**, *62*, 15006–15014.

[S6] W.-M. Wang, W.-T. Wang, M.-Y. Wang, A.-L. Gu, T.-D. Hu, Y.-X. Zhang, Z.-L. Wu, *Inorg. Chem.* **2021**, *60*, 9122–9131.

[S7] M. Singh, A. Karmakar, N. Seal, P. P. Mondal, S. Kundu, S. Neogi, *ACS Appl. Mater. Interfaces* **2023**, *15*, 24504–24516.

[S8] P. Meejaiyen, P. Pitakjakpipop, K. C. Stylianou, W. Anutrasakda, *Microporous Mesoporous Mater.* **2026**, *401*, 113941.

[S9] J. Gu, X. Sun, X. Liu, Y. Yuan, H. Shan, Y. Liu, *Inorg. Chem. Front.* **2020**, *7*, 4517–4526.